Comparison of 1D, coupled 1D–2D, and 2D shallow water numerical modeling for dam-break flow analysis of Way-Ela dam, Indonesia

Primerjava 1D, povezanega 1D–2D in 2D modeliranja plitvih voda za analizo pretoka ob porušitvi jezu Way-Ela, Indonezija

Metta Lim[1], Bobby Minola Ginting[1,*], Theo Senjaya[1], Christine Kieswanti [1]

[1] Department of Civil Engineering, Faculty of Engineering, Parahyangan Catholic University,
Jl. Ciumbuleuit No. 94, Bandung, 40141, Indonesia

Abstract

This study analyzes the flood inundation area using shallow water numerical modeling with HEC-RAS 6.3 software by comparing 1D, coupled 1D–2D, and 2D approaches. As a case study, the 2013 Way-Ela dam-break event in Indonesia is selected. Way-Ela Dam naturally formed by landslides in 2012, collapsed due to a piping mechanism after a heavy rainfall event. To estimate the breach outflow hydrograph, an empirical parametric model based on regression formula is used. Compared with the observed data, the numerical results show the 2D model produces the most accurate results among others, with reasonable computational time, while the 1D model, despite being computationally very efficient, misinterprets the flood extent map. The coupled 1D–2D model produces results similar to that of the 2D model; however, this coupled approach, which is expected to be more computationally efficient than the 2D one, interestingly yields a significantly longer calculation time. Some possible reasons are thus discussed. Additionally, comparisons for the water level and velocity are also presented in several locations to point out the difference between each model. Our finding informs the selection of an appropriate hydrodynamic model for dam-break simulations, balancing the result accuracy and computational cost.

Keywords: Dam-Break, HEC-RAS, Way-Ela, 1D modeling, coupled 1D–2D modeling, 2D modeling.

Izvleček

V tej študiji je analizirano območje poplavljanja z numeričnim modeliranjem plitvih voda s programsko opremo HEC-RAS 6.3, in sicer s primerjavo različnih pristopov: 1D, povezanega 1D–2D in 2D. Za študijo primera je izbran dogodek porušitve jezu Way-Ela v Indoneziji leta 2013. Jez Way-Ela se je naravno oblikoval zaradi zemeljskih plazov leta 2012, nato pa se je zaradi notranje erozije po močnem deževju porušil. Za oceno hidrograma odtoka ob porušitvi se uporablja empirični parametrični model, ki temelji na regresijski enačbi. Numerični rezultati v primerjavi z opazovanimi podatki kažejo, da 2D model podaja najnatančnejše rezultate, s sprejemljivim računskim časom, medtem ko 1D model, kljub časovni učinkovitosti izračuna, napačno

* Stik / *Correspondence*: bobbyminola.g@unpar.ac.id

izračuna obseg poplave. Povezani 1D–2D model poda podobne rezultate kot 2D model; vendar pa je pri povezanem pristopu čas izračuna bistveno daljši, čeprav se pričakuje, da bo računsko učinkovitejši od modela 2D. Podani so nekateri možni razlogi za to. Poleg tega so na več mestih predstavljene tudi primerjave za vodno gladino in hitrost in tako poudarjene razlike med različnimi modeli. Naše ugotovitve pomagajo pri izbiri ustreznega hidrodinamičnega modela za simulacije porušitve pregrad, pri čemer je treba poiskati pravo ravnovesje med natančnostjo rezultatov in stroški izračuna.

Ključne besede: porušitev pregrade, HEC-RAS, Way-Ela, 1D modeliranje, povezano 1D–2D modeliranje, 2D modeliranje.

1. Introduction

A dam is a lateral structure on a river that is built for several purposes, such as flood control, water management, irrigation, etc. A dam's capacity is determined by its contour and its levees' elevation, with a spillway to prevent water from overtopping. While dams are beneficial for humans and have high economic values, they are also potentially dangerous if they collapse, followed by hazardous floods that cause damage to the downstream area. Dams can generally be classified into two types based on origin: natural and constructed dams. While a constructed dam is designed with a spillway through a proper technical calculation, it is challenging to build a proper spillway for a natural dam since its features formed naturally through landslides, glacial ices, or moraines (Costa and Schuster, 1987).

According to information obtained from FEMA (2013), most dam failures are caused by overtopping (70.9%) and piping (14.3%), for both constructed and natural dams. Nevertheless, the failure potential of natural dams is higher than that of constructed dams due to porous and unconsolidated materials. In Indonesia, as the prevailing soil condition is unconsolidated, embankment dams are therefore prone to earthquakes (Awal et al., 2011). In addition, earthen and natural dams are at risk of overtopping and piping due to porous soils.

To the best of our knowledge, the first dam-break event in Indonesia was the Gintung Dam failure in 2009, which brought great losses to the downstream villages. Gintung Dam was built in 1933 and collapsed, releasing approximately 2 million m³ of water (Liputan 6, 2019). Some works that investigated the failure of Gintung Dam are noted;

see Ginting et al. (2013) and Nabilah et al. (2020). Despite a relatively low height of 6 m, reports indicated that there were 100 fatalities, around 100 people unaccounted for, and an area of 10 hectares downstream inundated due to the breaching of Gintung Dam. Since then, the Indonesian authority realized the importance of an Emergency Action Plan (EAP) to quantify the potential losses of dam-break events and consequently obliged the stakeholder of each dam in Indonesia to provide an EAP as a part of a dam operation permit.

The second dam-break event in Indonesia was the failure of Way-Ela Dam in 2013. In 2012, Way-Ela Dam came into existence as a natural dam. It was formed due to a cliff landslide, which effectively blocked the flow of the main river. However, it collapsed in 2013 due to heavy rainfall and released approximately 20 million m³ of water (BNPB, 2013a). Way-Ela Dam with an approximate height of 35 m, resulted in the unfortunate death of one person, the disappearance of another, and injuries to 32 people (Detik, 2013). Surprisingly, despite its larger size, Way-Ela Dam posed a lower risk than Gintung Dam. A contributing factor was that the EAP, a standard component in dam-break risk assessments, had not been fully implemented in Indonesia prior to the failure of Gintung Dam. Hence, conducting an in-depth analysis of dam-break risk assessments is crucial in mitigating threats to human lives, economic stability, and property damage, and prior to providing such an assessment, hydraulic analysis is required.

The propagation characteristics of dam-break flow have been studied for decades through several ways, e.g. analytical solutions, experimental, and numerical modeling. Among others, some pioneer works investigating the analytical solution of dam-

break flows include Ritter (1892), Dressler (1954), and Chanson (2006). The analytical solutions of dam-break events typically consider an infinite reservoir with a water level higher than the bed level downstream of the dam, where the dam-break phenomena are reconstructed by the dam's sudden removal. In the experimental and numerical studies of Benazir et al. (2019), it was discovered that the propagation of the dam-break wave was influenced by the reservoir depth and downstream depth. Similarly, Kobayashi and Uchida (2022) studied the propagation characteristics of breaking bores with various Froude numbers by means of experimental and numerical investigations.

Based on flow direction, hydraulic numerical modeling can be one-dimensional (1D), two-dimensional (2D), coupled 1D–2D, and three-dimensional (3D). While 3D models offer detailed outputs, they require complex processes and extensive computational time. In contrast, 1D models, with their simpler mathematical equations, are ideal for calculating flows in well-defined areas and are more accurate for in-channel hydraulics where water flows primarily in one direction (USACE, 2023a; Mark et al., 2004). 2D models can provide more detailed outputs than 1D models, especially for velocity distribution, and are suitable for complex floodplains and direct rainfall (rain-on-grid) modeling where water flows in both lateral and longitudinal directions; see Sebastian et al. (2022), Ginting et al. (2024), Ginting et al. (2023), Ginting and Ginting (2020), and Ginting (2019), among others. However, the simulation time needed for 2D models is relatively longer than that of 1D models, not only because the outputs of datasets are large (Gharbi et al., 2016), but primarily due to the dense numerical grids of 2D models compared to only the several cross sections used in 1D models.

Recently, it has been possible to couple 1D and 2D models, allowing for specific areas to be modeled using 1D while others utilize 2D. This is termed as an integrated approach to facilitate the connection between 1D and 2D models, dynamically representing interactions between the river and floodplain. Given the recent implementation of this 1D–2D coupling simulation, only a handful of researchers have explored its application in flood simulation analysis; see Dasallas et al. (2019), Patel et al. (2017), and Betsholtz and Nordlöf (2017). Therefore, the objective of this study is to compare the capability of shallow water modeling with HEC-RAS 6.3 software to simulate the flood propagation of the Way-Ela dam-break event by comparing 1D, coupled 1D–2D, and 2D models, so that the water depth, velocity, and inundation area can be compared against the observed data. In addition, the computational time of each approach will be compared. This study will be beneficial not only for practitioners but also the related stakeholders to choose the proper model in dam-break analysis.

2. Case Study: Way-Ela Dam

Way-Ela Dam was a natural dam formed by landslide due to heavy rainfall in 2012, located at 3°38'57.91'' S and 127°58'53.08'' E; see Figure 1. The dam's location was in Negeri Lima Village, Leihitu District, Central Maluku Regency, Indonesia. Based on Badan Nasional Penanggulangan Bencana (BNPB, 2013b), the dam's capacity reached 19.8 million m^3 with a crest length of 1,000 m and a height rom the terrain to the crest of 210 m. The dam was originally used for recreation and water management purposes (Suneth et al., 2016).

The technical data of Way-Ela Dam before the dam-break event is shown in Table 1. The dam collapsed a year later, on 25 July 2013, due to heavy rainfall. The embankment failed since the pressure given by the water was high enough to cause 42 piping spots to the embankment (BNPB, 2013b). The failure caused 1 fatality and 32 people wounded from 5,227 evacuees (BNPB, 2013a). An EAP that was composed in advance had avoided more fatalities and injuries. Figure 2 shows the inundation area caused by the Way-Ela dam-break event.

Figure 1: *Location of case study.*

Slika 1: *Lokacija študije primera.*

Figure 2: *Way-Ela Dam before (October 2012) and after (November 2013) the dam-break (Google Earth.)*

Slika 2: *Jez Way-Ela pred porušitvijo (oktober 2012) in po porušitvi (november 2013) (Google Earth).*

Table 1: *Technical data of Way-Ela Dam before the dam-break event.*

Preglednica 1: *Tehnični podatki za jez Way-Ela pred porušitvijo.*

Watershed Area	11.49 km^2
River Length	9.56 km
Dam Crest Level	+215 m
Normal Water Level (NWL)	+197 m
Reservoir Area (Estimated at NWL)	46.98 km^2
Reservoir Volume (Estimated at NWL)	19.8 × 10^6 m^3

3. Methodology

This study began by collecting the data to make the calculations needed for the hydraulics analysis, such as: (1) Digital Model Elevation (DEM); (2) breach outflow calculation based on Kieswanti (2023), and (3) the Manning coefficient values according to Bhola et al. (2018) and Ginting et al. (2024). After collecting the data, the hydraulics analysis, i.e. 1D, coupled 1D–2D, and 2D modeling, were carried out to obtain the simulation outputs such as water depth, velocity, and inundation area. The results were then compared and validated against the observed data. In the following sections, some parts, including the data, calculation formulas, and mathematical equations used in the analysis, are explained.

3.1 Digital Elevation Model (DEM)

Topographic data are one of the important inputs required in dam-break modeling. Ideally, fine-resolution, measured topographic data should always be used for hydraulic modeling as they represent the bare contours well. However, acquiring such data is costly and consumes much time and resources. Alternatively, open-access, satellite-derived DEM can be utilized for dam-break modeling. DEM is a dataset of topography conditions for a certain area of the earth. It is represented in XYZ values, where X and Y show the horizontal coordinate location and Z shows the elevation of a certain point.

There are several satellite-derived DEMs available as open-access data from coarser to finer-resolution, namely, the resolution of (a) ~90 m, i.e. MERIT (Multi Error Removed Improved Terrain)-Hydro, TanDEM-X (TerraSAR-X add-on for Digital Elevation Model); (b) ~30 m, i.e. SRTM (Shuttle Radar Topography Mission), ALOS (Advanced Land Observing Satellite); (c) ~8.1 m, i.e. DEMNAS (DEM Nasional). Note that not each DEM is suitable for hydraulic modeling, as it may sometimes misinterpret the actual topography conditions, for instance, DEMs with a type of Digital Surface Model (DSM) detects object surfaces (e.g. water, roofs, trees, etc.) as bare contours. Meanwhile, a Digital Terrain Model (DTM) removes object surfaces and only detects ground contours; it is therefore more suitable for hydraulic modeling.

This work used ALOS, which was launched by the Japan Aerospace Exploration Agency (JAXA). This DEM was generated by the Panchromatic Remote-sensing Instrument for Stereo Mapping (PRISM) with 2.5 m spatial resolution. ALOS was chosen because it has high precision for vertical resolution (< 5 m), supported by PRISM, AVNIR-2, and PALSAR technologies, as well as the stereoscopic images at multiple views (nadir, backward, and forward); see Bettiol et al. (2021), Takaku et al. (2020), and The Japan Aerospace Exploration Agency (JAXA) (2006). Therefore, despite a horizontal resolution of ~30 m, it gives accurate representation of the terrain for our study.

Other studies also showed that ALOS could produce accurate results for hydrologic-hydraulic applications. In certain regions around the globe like Estonia, Norway, New Zealand, and China, ALOS was able to attain the highest vertical accuracy of all DEMs; see Uuemaa et al. (2020). In Tesema (2021), ALOS and SRTM produced similar watershed parameters in Ethiopia but the former yielded more accurate results for peak discharge computation. In Chymyrov (2021), ALOS was shown to have higher vertical accuracy than SRTM for hydrology analysis in the mountainous region in Kyrgyzstan.

Recently, ALOS was shown in Ginting et al. (2024) to be significantly more accurate than other four DEMs, i.e. DEMNAS, SRTM, TanDEM-X, and MERIT-Hydro to compute the flood hydrograph in the Katulampa watershed, Indonesia. Note that the finer-resolution DEM like DEMNAS was not

accurate for hydrologic-hydraulic applications because it is basically derived as a DSM type that detects object surfaces as ground contours, thus being not suitable for flow analysis.   The terrain elevation represented by ALOS for this study is shown in Figure 3.

3.2 HEC-RAS

The hydraulic analysis is carried out using Hydrologic Engineering Center's River Analysis System (HEC-RAS) 6.3 software. It has the capability of performing 1D, coupled 1D–2D, and 2D modeling. Additionally, it also has a feature to estimate breach outflow hydrograph. Each part is briefly explained in the following sections.

3.2.1   Breach Outflow Computation

An essential consideration in this study involves analyzing the breach flow hydrograph, which serves as the primary input to investigate the flood inundation. Previous research has extensively investigated breach characteristics in both earthen and rock-filled dams, encompassing phenomena

such as overtopping, piping, sliding, and wave actions, resulting in several empirical formulas; see Singh and Snorrason (1984), MacDonald and Langridge-Monopolis (1984), Von Thun and Gillette (1990), Froehlich (1995), Chinnarasri et al. (2004), Froehlich (2008), Xu and Zhang (2009), and Lorenzo and Macchione (2014), among others.

Table 2: Regression data range for the empirical formulas

Preglednica 2: *Obseg regresijskih podatkov za empirične enačbe*

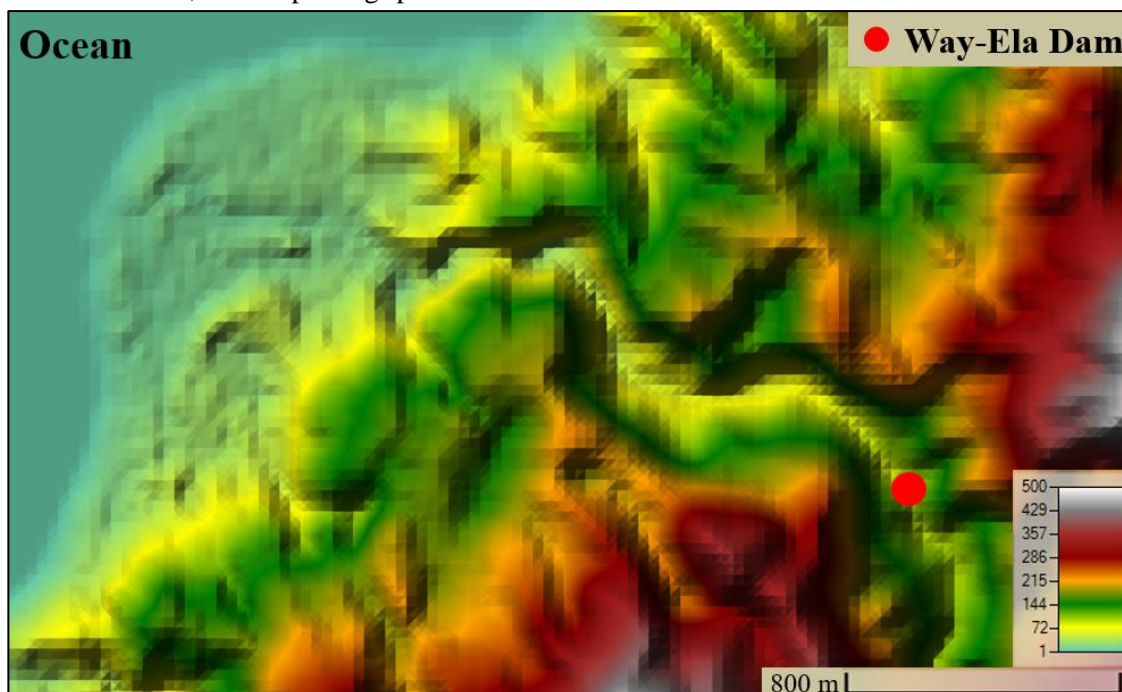|	Height of the dams (m)	Volume of water at breach time (million m^3)
MacDonald & Langridge-Monopolis	4.27–92.96	0.0037–660.0
Froehlich	3.05–92.96	0.0139–660.0
Von Thun & Gillette	3.66–92.96	0.027–660.0
Xu & Zhang	3.2–92.96	0.105–660.0

Figure 3: *Way-Ela Dam terrain in HEC-RAS.*

Slika 3: *Teren jezu Way-Ela v HEC-RAS.*

HEC-RAS 6.3 employs some of these empirical formulas (e.g. MacDonald & Langridge-Monopolis, Von Thun & Gillette, Froehlich, and Xu & Zhang) to determine the critical breach parameters such as peak breach discharge, total breach formulation time, and the ultimate breach shape. Generally, these formulas were of regression equations derived from several dam-break events around the world; see the resume in Table 2 based on USACE (2016). While such formulas only determine the critical breach parameters, the progression of breach development from its initial phase to the final stage remains elusive, however. Hence, there are two ways to define the breach progression in HEC-RAS 6.3: (1) by assuming a linear or sine progression corresponding to the total breach formulation time and (2) manually defined by the users.

Note that we only focus in this study on comparing 1D, coupled 1D–2D, and 2D modeling of flood propagation due to the Way-Ela dam-break event, and we therefore follow the results of Kieswanti (2023), in which the formula by Von Thun & Gillete could produce the most accurate result, inter alia by assuming a linear breach progression corresponding to the total breach formulation time. The concept of a linear breach progression can be seen in Yudianto et al. (2021). We write the Von Thun & Gillete formula as:

$$B_{ave} = 2.5\, h_w + C_b \qquad (1),$$

where B_{ave} is the breach average width (m), h_w is the water depth calculated from the bottom of the breach (m), and C_b is the reservoir size coefficient given in Table 3. The final breach shape is assumed to be a trapezoid with a breach side slope of 1H:1V, except for dams with cohesive soils; the side slopes are in between 0.5H:1V to 0.33H:1V (H and V denote horizontal and vertical, respectively).

The total breach formulation time t_f (hour) is calculated as:

$$t_f = 0.02\, h_w + 0.25 \qquad (2)$$

$$t_f = 0.015\, h_w \qquad (3)$$

The two above equations are for erosion-resistant and easily erodible materials, respectively. Assuming the breach progression is linear to the value of t_f, the breach outflow hydrograph can be calculated in HEC-RAS 6.3.

Table 3: *Reservoir size coefficient (C_b).*

Preglednica 3: *Koeficient velikosti zbiralnika.*

Reservoir Size (m³)	C_b
<1.23 x 10⁶	6.1
1.23 x 10⁶–6.17 x 10⁶	18.3
6.17 x 10⁶–1.23 x 10⁷	42.7
>1.23 x 10⁷	54.9

The information from BNPB (2013a) and that mentioned in Wisyanto and Naryanto (2022), namely of observations of the reservoir's water surface level and rainfall since 1 July 2013, indicate that it reached an elevation of +188 m. Subsequently, on 9 July, the water level rose to +189 m. The situation worsened with the continuous increase in the water level and, by 25 July, the water elevation had reached +196.6 m. At 02:05 am (local time) on 25 July, water began to overflow from the dam body, and by 12:05 pm, the dam had completely collapsed.

In accordance with this information, Kieswanti (2023) estimated the breach outflow using a 1D model in HEC-RAS. A storage area representing the Way-Ela reservoir was connected with an inline structure representing the dam and the river cross sections extracted from the DEM approximately 10 m downstream of the dam. The vertical reference of the DEM was adjusted to closely follow the reservoir datum. The upstream boundary condition was the flood hydrograph (computed from 432 mm/day of rainfall) flowing to the storage area. The initial piping hole elevation was set to +196 m (an estimated value to closely follow the field condition), where the breach progression was assumed to be linear. The downstream boundary condition was set to a normal depth condition.

The breach outflow hydrograph computed is shown in Figure 4. It can be noted that the outflow initially existed at around 02:00 am and the breach was completely formed after approximately 40 mins (time-to-peak). The peak discharge reached 5,248.40 m³/s. This result is in accordance with the chronology described in Wisyanto and Naryanto (2022).
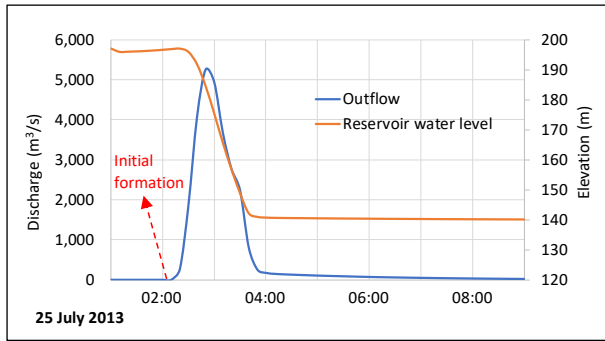

Figure 4: *Breach outflow hydrograph* (Kieswanti, 2023).

Slika 4: *Hidrogram odtoka ob porušitvi* (Kieswanti, 2023)**.**

Several previous studies had also computed the breach outflow for the Way-Ela dam-break event as follows: in Rachmadan et al. (2014), the breach outflow for this event was computed using ZHONG-XING HY21 software for different breaching scenarios (i.e. overtopping and piping mechanisms), yielding the peak values within a range of 2,132–7,089 m3/s. In Yakti et al. (2019), the breach outflow was estimated using HEC-HMS software for some similar scenarios, resulting in the peak values ranging from 9,280–13,698 m³/s. In Kieswanti (2023), however, the breach outflow was estimated only for a piping mechanism in accordance with the aforementioned information from BNPB (2013a) and Wisyanto and Naryanto (2022).

3.2.2 1D, Coupled 1D–2D, and 2D Modeling

HEC-RAS 6.3 solves the shallow water (St. Venant) equations for all numerical modeling. For 1D simulations, the velocity is assumed to be uniformly distributed in the vertical (over the channel depth) and transversal (over the channel width) directions. The 1D governing equations in x direction (m) and over time t (s) are written as follows:

$$\frac{\partial A}{\partial t} + \frac{\partial Q}{\partial x} = 0 \tag{4}$$

$$\frac{\partial Q}{\partial t} + \frac{\partial (QV)}{\partial x} + gA\left(\frac{\partial \eta}{\partial x} + S_f\right) = 0 \tag{5},$$

where A is the cross-sectional wetted area of channel (m²), Q is the flow discharge (m³/s), V is the flow velocity (m/s), η is the water surface elevation (m), and S_f is the friction slope term. Equation (4) denotes the mass conservation, whereas Equation (5) expresses the momentum conservation. There are two options of solver for 1D modeling in HEC-RAS 6.3, namely finite difference and finite volume methods. The latter was used for our study.

For 2D simulations, the distribution of velocity is assumed to be vertically uniform, but the transversal velocities are computed in x and y directions over time t based on the spatial discretization. Two options are available in HEC-RAS 6.3 for 2D modeling, namely the Eulerian-Lagrangian Shallow Water Equation (EL-SWE) and Diffusive-Wave Equation (DWE) solvers; both are solved within a framework of finite volume method. Contrary to DWE, the EL-SWE solver can calculate the local and convective acceleration (USACE, 2023b), and was therefore employed in our work. Neglecting the turbulence and Coriolis terms, the 2D governing equations are expressed as follows:

$$\frac{\partial h}{\partial t} + \frac{\partial (hu)}{\partial x} + \frac{\partial (hv)}{\partial y} = 0 \tag{6}$$

$$\frac{\partial u}{\partial t} + u\frac{\partial u}{\partial x} + v\frac{\partial u}{\partial y} + g\frac{\partial \eta}{\partial x} + \frac{\tau_{b_x}}{\rho R} = 0 \tag{7}$$

$$\frac{\partial v}{\partial t} + u\frac{\partial v}{\partial x} + v\frac{\partial v}{\partial y} + g\frac{\partial \eta}{\partial y} + \frac{\tau_{b_y}}{\rho R} = 0 \tag{8},$$

where h is the water depth (m), u is the velocity in x direction (m/s), v is the velocity in y direction (m/s), η is the water surface elevation (m), τ_{b_x} and τ_{b_y} are the bottom shear stresses in x and y directions, respectively (kg m⁻¹ s⁻²), R is the hydraulic radius (m), and ρ is the density (kg/m³).

Generally, the 1D model is preferable for analyzing the flow and water level in channels, where the water mainly flows in one direction. In this regard, the floodplain produced by 1D analysis is defined by the subtraction of the topographic data with the water surface elevations (Cook, 2008). Unlike 1D

models, 2D models are suitable for hydraulic analysis with large geographical areas. The lateral and longitudinal direction calculations of 2D modeling can give better outputs in large and coarse surfaces areas. The 2D computational meshes help produce a continuous floodplain, which is more accurate than a floodplain derived by 1D modeling.

In principle, 2D modeling requires more computational time than the 1D modeling, and hence, the idea of coupled 1D–2D model emerged to have the advantage of 1D and 2D models to produce better results with less computational time. In HEC-RAS 6.3, a coupled 1D–2D model requires the same input data as a 2D model. There are two different ways to conduct simulations with a coupled 1D–2D model in HEC-RAS 6.3 (Betsholtz and Nordlöf, 2017). The first involves establishing a lateral connection, where 2D flow areas are linked to 1D cross sections using lateral structures. The second entails modeling the upstream (or downstream) segment of the river exclusively in 1D and connecting the furthest downstream (or upstream) cross section with a 2D area. In this work, the latter was employed.

3.2.3 Manning Coefficient Value

As previously described by the friction term S_f in Equation (5) as well as the term τ_{b_x} and τ_{b_y} in Equations (7) and (8), both 1D and 2D modeling with HEC-RAS 6.3 require bed roughness values, which are accounted for by means of the Manning formula. To this regard, the Manning coefficients are determined based on the land use map, where the domain is divided into three land use types, namely water bodies, urban area, and forest; see Figure 5. The Manning coefficient value for each land use type is set according to Bhola et al. (2018) and Ginting et al. (2024), who proposed calibrations of such values for hundreds of simulations; see Table 4.

In Bhola et al. (2018), the Manning coefficients were validated for an urban flood case in Germany by comparing the simulated depth with the observed data considering unsteady flood hydrographs, where buildings were excluded from the computational cells. In Ginting et al. (2024), urban areas were simulated by setting larger Manning coefficient values for ran-on-grid modeling and validated by comparing the computed and measured flood hydrograph at the given outlet.
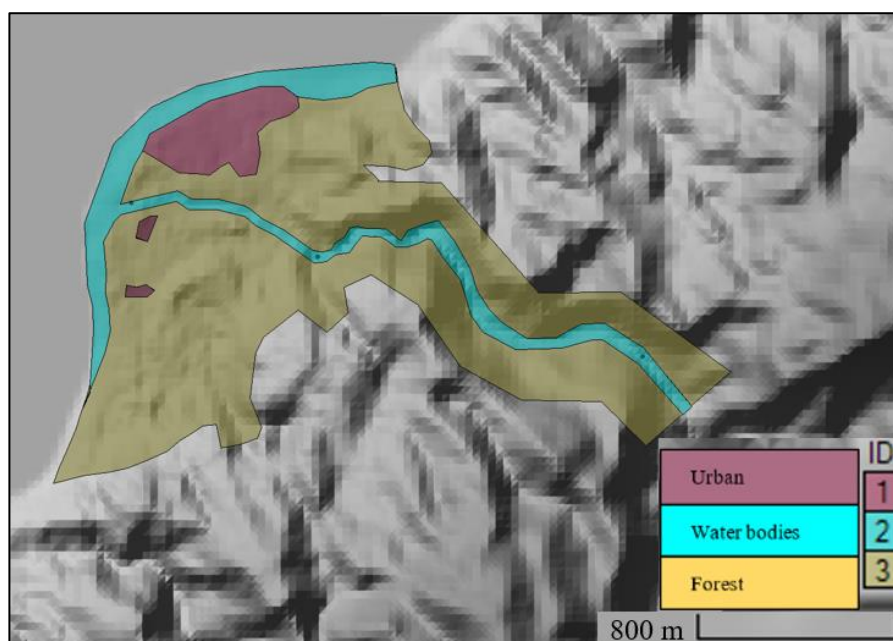

Figure 5: *Manning coefficient distribution map.*

Slika 5: *Porazdelitev Manningovega koeficienta.*

Table 4: *Manning coefficient value for each land use type.*

Preglednica 4: *Vrednost Manningovega koeficienta za vsako vrsto rabe zemljišča.*

Land Use	Calibrated Manning's n (s/m$^{1/3}$)
Water bodies	0.022
Forest	0.189
Urban	0.074

3.3 Observed Data and Previously Computed Results

The numerical results will be validated against the observed data, that is, the inundation area processed with QGIS software from the orthophoto of an inundation image after the Way-Ela dam-break event, obtained from BNPB (2013b); see Figure 6. According to BNPB (2013b), the average flood depth and average flood velocity due to the Way-Ela dam-break event were predicted to be 20 m and 11 m/s, respectively. However, no other details can be found on how these values were obtained.

Note that only the observed inundation data was officially available from the authority. However, we also note here the study of Salahuddin et al. (2021), which computed the average flood depth and average flood velocity during the dam-break event as 24 m and 10.98 m/s, respectively, at the middle of the inundation area (approximately 2.5 km from the ocean upstream). This was done by means of the Manning formula. All these findings were used in our study for comparison purposes.

4. Results

4.1 Computational Domain and Setting

As previously mentioned, we utilize ALOS in our work to gather topographic data for 1D, 2D, and coupled 1D–2D modeling, represented by cross sections, finite volume meshes, and a combination of both, respectively. In this section, we explain the computational domain for each modeling. For 1D modeling, some cross sections are generated approximately within an interval of 10 m, depending on the river curves, following the river path to the ocean along 2,860 m. The cross sections are configured to cover the main river and riverbank areas. In the coastal zones, the cross sections are created in such a way that they cover the residential areas.
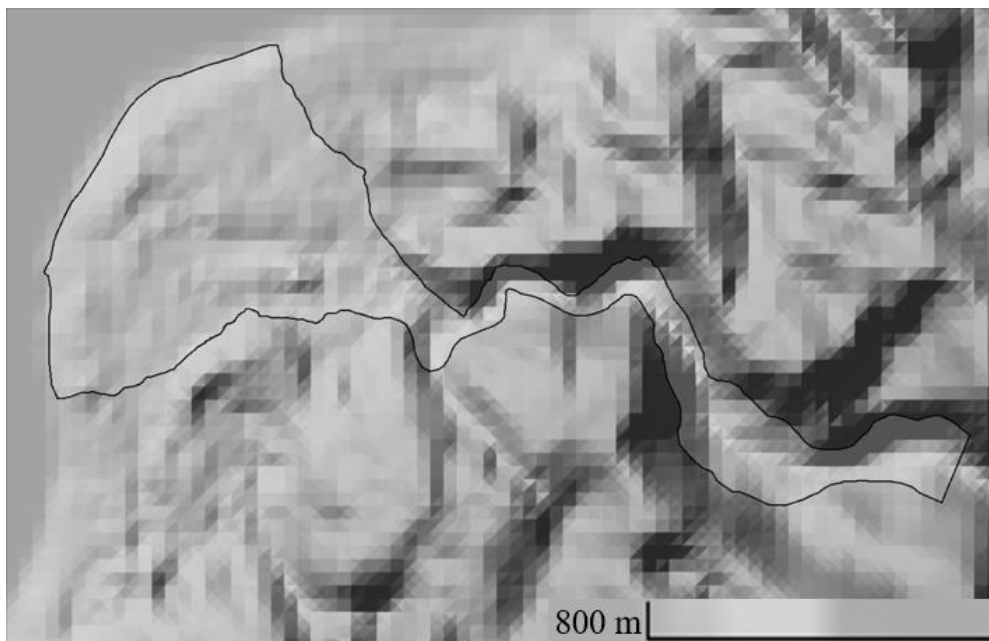

Figure 6: *Observed inundation data.*

Slika 6: *Zabeleženi podatki o obsegu poplave.*

For 2D modeling, the domain boundaries are determined to cover the hilly regions (upstream) and the residential areas, which are confined by the coastline. Meshes with a size of 10 m are used. For coupled 1D–2D modeling, we define the 1D domain for the upstream part using the same cross section data with 1D modeling, where the computational domain for the downstream part is set in accordance with the boundary for 2D modeling. As previously

mentioned, we employed a direct connection between the 1D river reach and 2D flow area. The 1D domain is applied to the narrow river section (upstream), while the 2D domain is used downstream. In this case, the water flowing from the 1D domain is distributed within the 2D area based on the conveyance distribution in the connected cross section, and the flow propagation is then modeled using the 2D model.
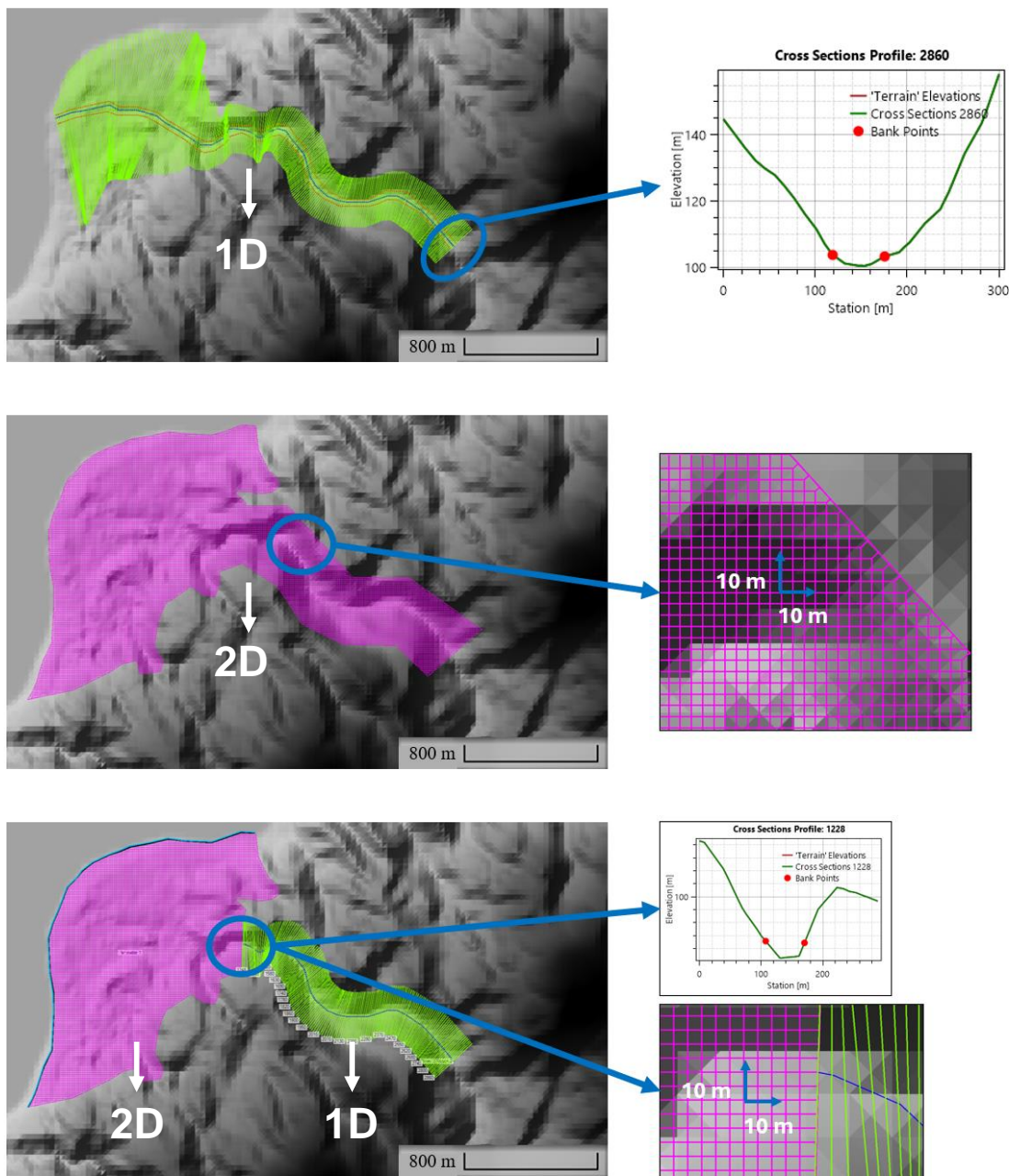

Figure 7: *A comparison of 1D, 2D, and coupled 1D–2D computational domains.*

Slika 7: *Primerjava računskih domen 1D, 2D in povezane 1D–2D.*

Note that it is also possible to do this the other way around, for instance by setting 2D boundaries for the upstream part and 1D cross sections for the downstream part. However, we did not do this because we consider 1D model to be more appropriate for the narrow river sections than 2D model. This is in accordance with USACE (2023b), which recommends this approach, where flows are dominantly 1D. A comparison of 1D, 2D, and coupled 1D–2D computational domains is shown in Figure 7.

Initially, the domain is in dry condition without any water downstream of the dam. Hence, to suit the natural river condition (before the dam-break event), we perform first the simulation with a base flow value. This is done by extending the flood hydrograph in Figure 4 with a constant discharge of 50 m^3/s for 5 hours, which subsequently produces initial depth and velocity values along the river to the ocean. The boundary condition at the ocean is set with an energy slope for the normal depth value in HEC-RAS. In fact, there were water surface fluctuations due to tidal forcing; however, these data were not considered in all our simulations since we were not able to acquire them. In addition, the effect of water surface fluctuations on the flood characteristics due to dam-break is insignificant and thus can be neglected.

In HEC-RAS 6.3, the bed roughness is accounted for by the Manning formula. For 2D modeling, the Manning coefficient values are assigned to the computational meshes using polygons as shown in Figure 5. Meanwhile, the Manning coefficient values for 1D modeling are assigned for each cross section that vary along the cross-section coordinates based on the values shown in Figure 5. Note that, as no detailed field measurement was available, it is difficult to precisely define the positions of the left and right riverbanks. Therefore, we assume an average river width of 70 m following Salahuddin et al. (2021).

Figure 8 illustrates the process of determining the values of the Manning coefficient for 1D modeling. It is shown that there are four segments with different Manning coefficient values at one cross-section. Hence, HEC-RAS calculates a composite value for this. The calculation interval was

established at 1 s (with a fixed time step) for 1D, 2D, and coupled 1D–2D simulations, and the entire simulation spanned 12 hours, giving the maximum Courant number within a range of 0.92–0.95 for each modeling. All standard parameters were used, including a water depth tolerance of 0.003 m.
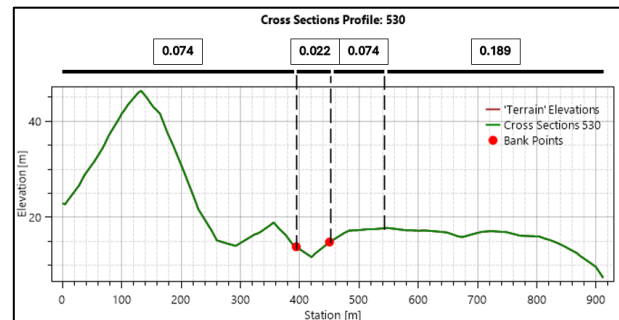

Figure 8: *Determining the Manning coefficient values for 1D modeling.*

Slika 8: *Določanje vrednosti Manningovega koeficienta za 1D modeliranje.*

4.2 Comparison of Inundation Area

In this section, the results of inundation area are first presented and compared with the observed data; see Figure 9. One can see that for the narrow river sections (upstream), each model shows similar results and almost no significant differences are observed. Meanwhile, in the middle (especially at the bending part), all models overestimate the inundation area.

The notable differences can be seen at the downstream part, where the 1D model becomes significantly less accurate than other models by underestimating the inundation area at the southern part but overestimating it at the northern area. Meanwhile, both 2D and coupled 1D–2D models can predict the inundation area more properly. At the southern area, both models overestimate the inundation area but still yield a better result than the 1D model.

Note that the discrepancies in the middle part may be caused not only by the capability of the models but also be due to the DEM resolution that cannot capture the river bends appropriately, thus influencing the results of each model. Therefore, acquiring precise measurements of topographic data at fine resolutions is desirable but was not possible for our study, unfortunately.
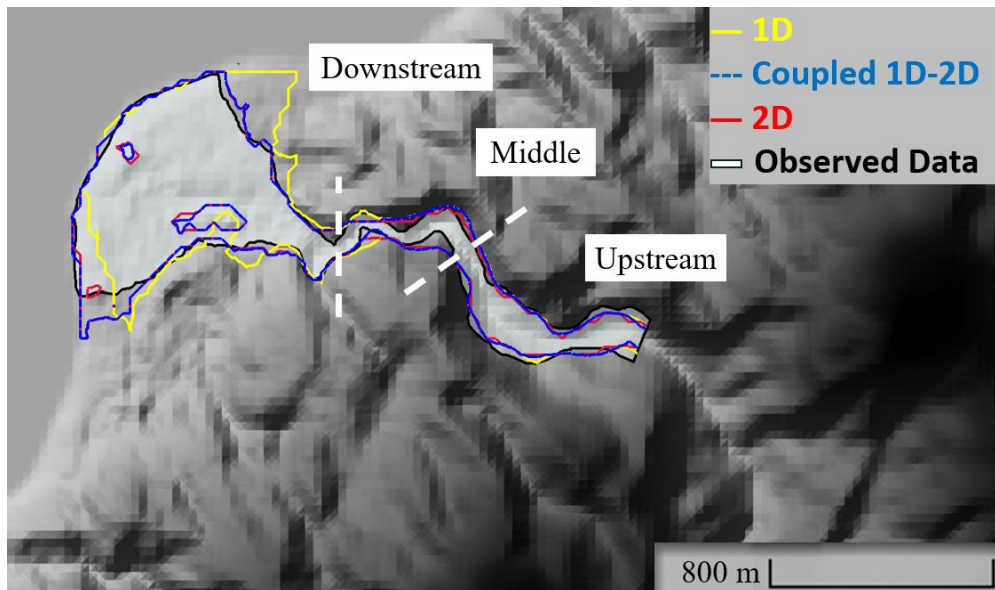
Figure 9: *Comparison of inundation area.*

Slika 9: *Primerjava poplavnega območja.*

4.3 Comparison of Depth and Velocity

The results of depth and velocity values between each model were nonetheless compared. In this regard, the maximum depth and maximum velocity during the simulation time are presented. As the range of depth values between the upstream and downstream parts is large, we thus use two color patterns to point out the differences; see Figure 10. The first pattern is of a range between 1–50 m (the values larger than 50 m are colored the same) and the second one is 1–10 m (the values larger than 10 m are colored the same).

It can be noted from the first color pattern that all models exhibit similar behaviors in the upstream part. In the middle part, depths of (more than) 50 m are shown to concentrate on the river bend by all models. However, the 1D model thereafter shows different values from others. This indicates significant differences of results between the 1D computational domain computed solely using the 1D model and the one with the coupled 1D–2D one.

According to our investigations, such differences are attributed in the 1D model due to the numerical computation for the river bend, as though it blocks the flow and results in higher depths downstream.

Meanwhile, using the coupled 1D–2D model reduces water obstructions in the middle part and, therefore, produces lower water depths downstream, although the numerical computation is still performed using the 1D model there. Probably, the numerical treatment of the coupled 1D–2D model at the interface between the 1D and 2D domains has ensured that the water predominantly flows downstream (to the 2D computational area). This is noticed from the condition that the maximum depth of the coupled 1D–2D model also reaches 50 m in the river bend, indicating a maximum value similar to the 1D model but with different values thereafter.

From the second color pattern in Figure 10, it can be observed that both coupled 1D–2D and 2D models again exhibit similar results for the downstream parts. The flood depth values around the coastal area are within a range between 1–3.5 m. It can be seen that there is no region around the coastal zone suffering from floods with a depth of more than 3.5 m. Meanwhile, the 1D model produces depths within a range of 1–8.5 m; it becomes even higher (more than 10 m) in the coastal zone.
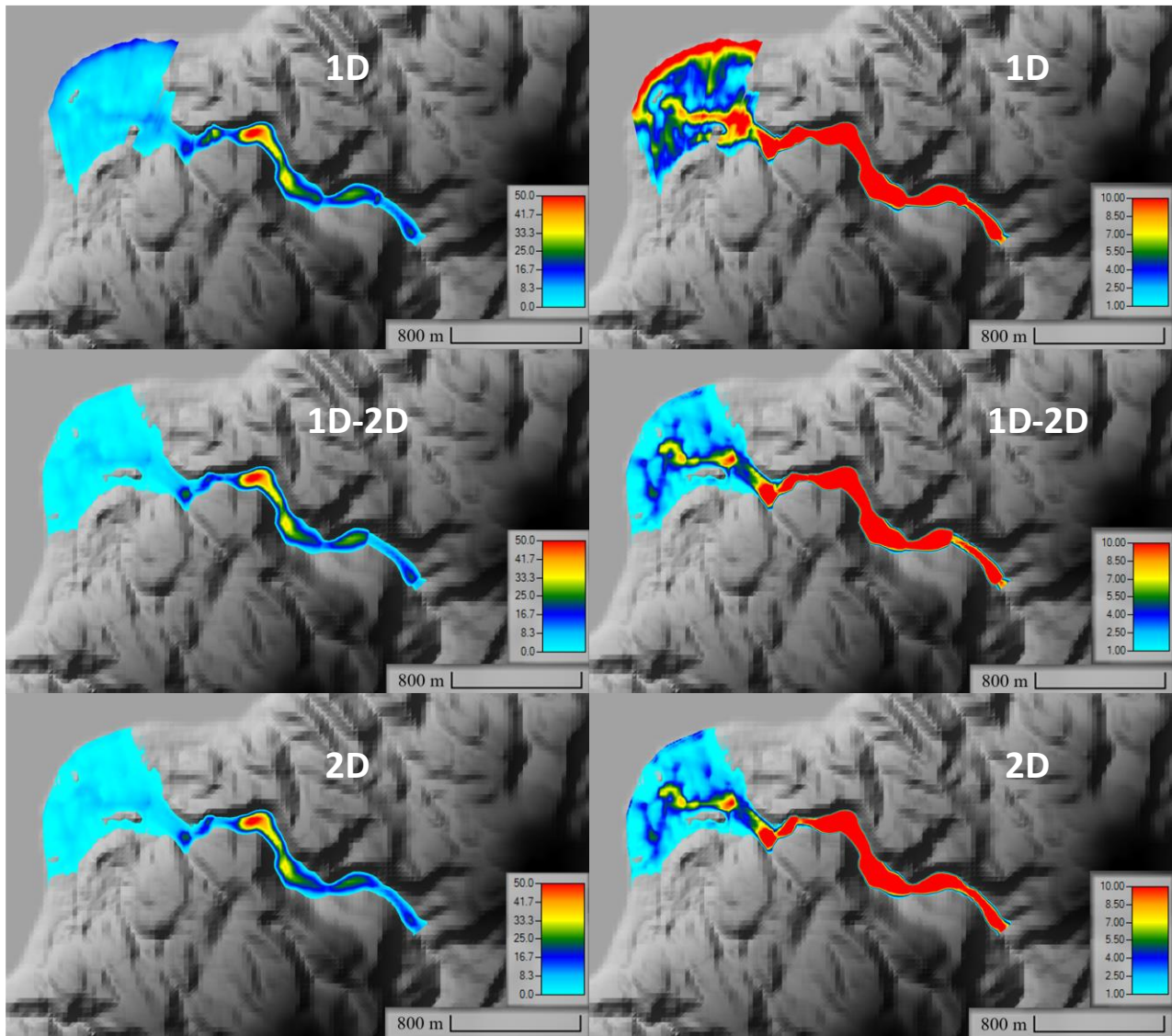
Figure 10: *Comparison of maximum depth with different color patterns: 1–50 m (left) and 1–10 m (right).*

Slika 10: *Primerjava največje globine z različnimi barvnimi vzorci: 1–50 m (levo) in 1–10 m (desno).*

A comparison of the maximum velocity is presented in Figure 11. Albeit insignificant, velocity differences can be noticed between the results of the coupled 1D–2D and 2D models along the narrow river sections. The former tends to produce higher velocities in the riverbank than does the latter, while the difference becomes more evident in the river bend. The coupled 1D–2D model shows relatively similar results to the 1D model along the narrow river sections, where both models give similar depth values there, as previously shown in Figure 10. At the downstream part, both coupled 1D–2D and 2D models show similar velocities but significantly different values from the 1D model. The 1D model yields lower velocities around the residential areas, as the depth values computed there are significantly higher than elsewhere.
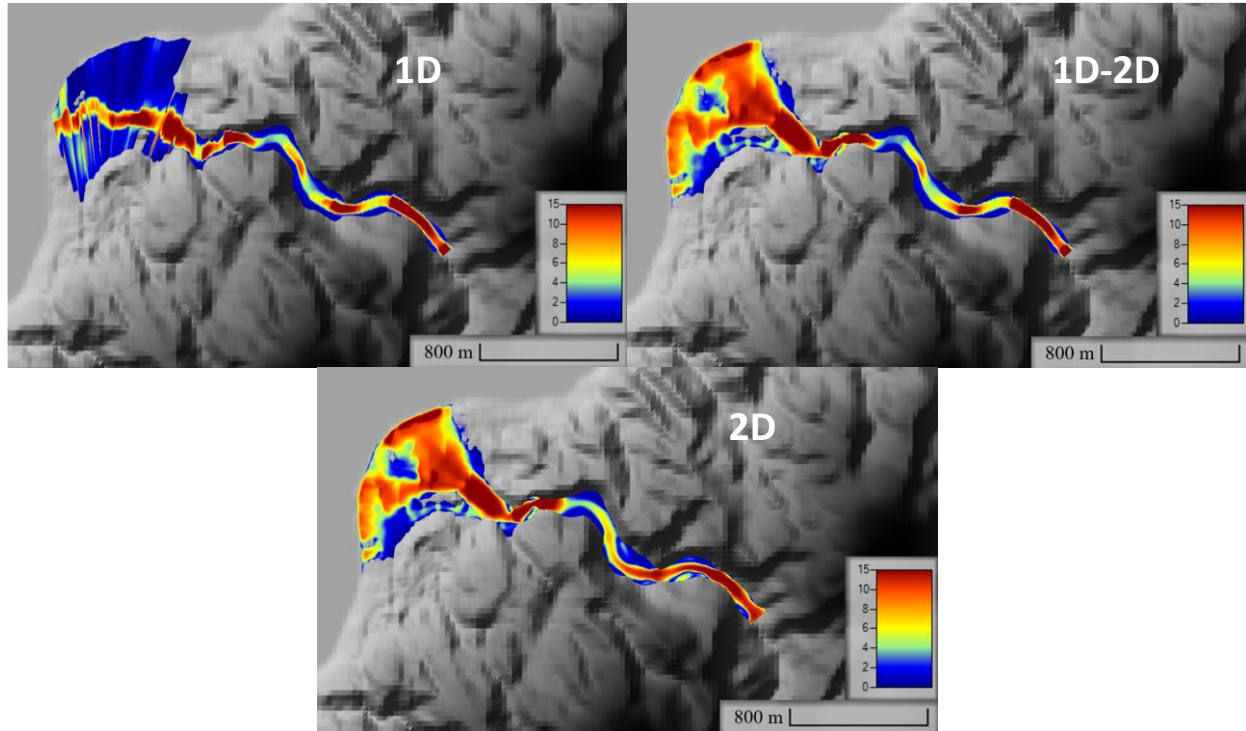
Figure 11: Comparison of maximum velocity (legend in m/s).

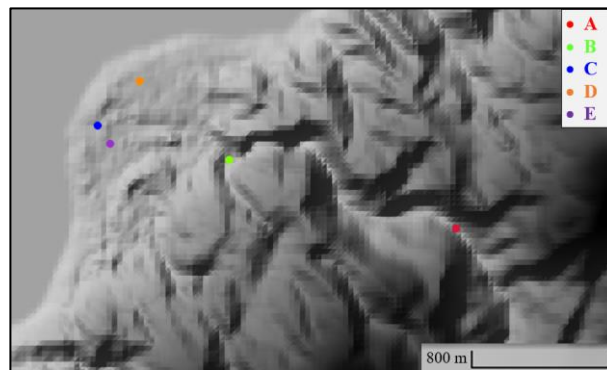*Slika 11: Primerjava največje hitrosti (legenda v m/s).*

Figure 12: Location of points A, B, C, D, and E.

Slika 12: Lokacija točk A, B, C, D in E.

4.4 Comparison of Time Series of Depth and Velocity

In this section, we compare the time series of depth and velocity at five points (A, B, C, D, and E) within the inundation area; see Figure 12. The coordinates of these points are described in Table 5. Points A and B represent the narrow river section (upstream) and the interface between the 1D and 2D models, respectively. Point C represents the river part at the coastal zone, while points D and E represent the residential areas (downstream). Note that these points are selected only for comparison purposes.

Table 5: Coordinate of points A, B, C, D, and E.

Preglednica 5: Koordinate točk A, B, C, D in E.

Points	x (m)	y (m)
A	387154.11	9596489.27
B	385865.43	9596886.09
C	385115.27	9597082.83
D	385351.10	9597334.26
E	385185.84	9596978.56

Lim M.: Comparison of 1D, coupled 1D–2D, and 2D shallow water numerical modeling for dam-break flow analysis of
Way-Ela dam, Indonesia – Primerjava 1D, povezanega 1D–2D modeliranja plitvih voda za analizo pretoka ob porušitvi
jezu Way-Ela, Indonezija
Acta hydrotechnica **37/66 (2024)**, 27–50, Ljubljana
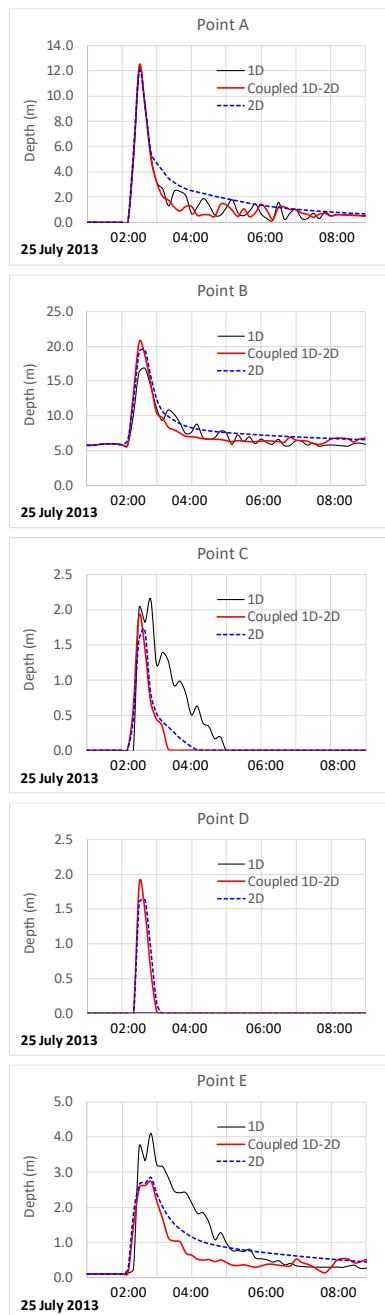
Figure 13: *Comparison of depth time series at points A, B, C, D, and E.*

Slika 13: *Primerjava spreminjanja globine s časom v točkah A, B, C, D in E.*

The comparison of depth time series is shown in Figure 13. All models can capture the arrival time of the incoming wave similarly at point A. The maximum depths computed using the three models are similar, but the recession part shows different values, where the 2D model produces larger depth values. The results of the coupled 1D–2D model oscillate for the recession part like the 1D model, as

expected. At point B, both coupled 1D–2D and 2D models compute the depth within a value range of 20–21 m, which is somehow in accordance with the results in Salahuddin et al. (2021). Meanwhile, the 1D model computes it approximately by 4 m lower of water depth.

Oscillations again exist at point B from the 1D model for the recession part; however, no oscillations are detected from others. At points C and E, both coupled 1D–2D and 2D models produce similar maximum depth values but again the latter gives higher water depth for the recession part, whereas the 1D model keeps exhibiting oscillations. Interestingly, all models show similar behaviors at point D, and no oscillations are observed.

In Figure 14, the comparison of velocity time series is presented. Both 1D and coupled 1D–2D models exhibit very similar velocity values at point A. At point B, the 1D model produces lower velocities than others. Oscillations exist from the 1D model, which are stronger and more chaotic than those for the depth results. At point C, the 1D model yields higher velocities, despite giving higher depths than others. We also observe that the 1D model computes significantly lower velocities than others at point E in accordance with the depth results yielded. Finally, we notice that all models produce similar maximum velocity values at point D. All these findings indicate that both coupled 1D–2D and 2D models exhibit similar results (except for the recession part) but the results of the 1D model differ significantly.

We believe that the oscillations in Figure 13 and Figure 14 are related to the numerical treatment that subsequently affects computational stability, and this is a common issue in 1D unsteady flow modeling with HEC-RAS. Generally, 1D HEC-RAS model prefers gradual changes (for both topography and inflow data), which are contrary to the nature characteristics of dam-break flows. The flow properties, i.e. water level and velocity, are computed in the 1D model using the HTab parameter feature that generates curves for conveyance, storage area, and flow area based on an increment vertical section for each cross-section data.
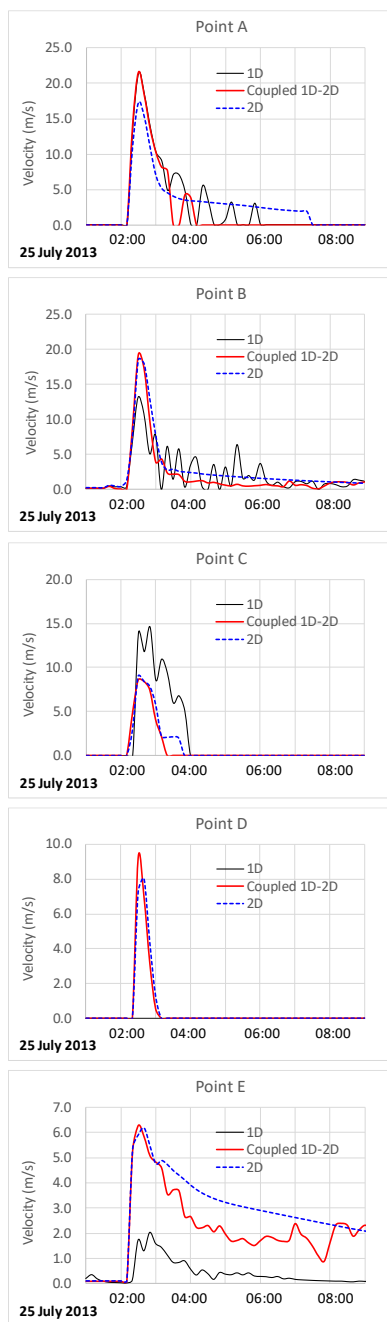
Figure 14: *Comparison of velocity time series at points A, B, C, D, and E.*

Slika 14: *Primerjava spreminjanja hitrosti s časom v točkah A, B, C, D in E.*

During computations, the 1D model selects and interpolates values from such curves, instead of calculating the hydraulic parameters for each time step. Hence, this interpolation process may cause oscillations when dealing with rapidly varying unsteady flow. Meanwhile, the 2D model in HEC-RAS is supported by the recent finite volume shock-capturing scheme that allows for more stable results.

The flow properties in the 2D model are directly computed for each time step based on flux conservation. Note that the aforementioned issue in the 1D model may become the cause of oscillations for the coupled 1D–2D model accordingly.

4.5 Comparison of Computational Time

The computation durations exhibit significant differences across the 1D, coupled 1D–2D, and 2D models. In our work, the 1D model renders the simulation for the entire model area over a 12-hour long period in a couple of seconds, whereas the 2D model requires minutes to finish the simulation. Surprisingly, the coupled 1D–2D model, which is expected to be more efficient than the 2D model, needed significantly longer computational time than the others. The computational time is summarized in Table 6.

Table 6: *Computational time comparison.*

Preglednica 6: *Primerjava računskih časov.*

Model	Computational Time (hh:mm:ss)
1D	00:00:28
Coupled 1D–2D	01:03:51
2D	00:21:36

5. Discussion

5.1 Result Accuracy

Despite its main advantage of significantly less computational time, the 1D model has several shortcomings arising from the simplification of real physical processes. For instance, it is not possible to account for overland flow that dominantly exists at the downstream part. Another disadvantage of using the 1D model is the fact that it only computes a single water surface for each cross section at a certain time, which accordingly affects the inundation dynamics. This can be seen in Figure 9, where the 1D model misinterprets the inundation area downstream.

To increase the accuracy of 1D modeling, Betsholtz and Nordlöf (2017) suggested adding levees to restrict specific portions of the cross section so that the flow characteristics in the main channel section

could be more properly computed, at least before the water overtops such levees. According to our experience, this approach, however, does not play a significant role for our work because the dam-break flow increases the water level rapidly, and as soon as the water reaches the crests of the levees, the overbank area is flooded instantaneously.

A more detailed examination is needed to understand the differences between the coupled 1D–2D and 2D models in the context of modeling channel flow and the interaction between the channel and the floodplain. In this regard, one should understand that the displayed results of the 1D model in the RAS-mapper or any Geographic Information System (GIS) platforms are interpolated from cross-section locations to a continuous surface and the superimposed on a terrain model. Obviously, it may significantly influence the final flood maps. In our work, it is likely to occur in the 1D model results; see Figure 10 at the northern part of the modeled domain downstream.

Another important aspect worth pointing out is that the velocity distribution map of the 1D model results is generated solely based on the interpolation of cross-section values (USACE, 2016). This also means that it is impossible to map velocities around any features represented between cross-sections, unless by means of interpolation. In this work, it was not feasible to estimate proper velocity values around terrain conditions especially for the downstream area. This becomes evident in Figure 11, where there is a gap of velocity value at the northern part of the modeled domain downstream. The mapped velocity is hence unrealistic. This finding is in accordance with the outputs obtained in other previous studies, e.g. Betsholtz and Nordlöf (2017), Vojinovic and Tutulic (2009), and Tayefi et al. (2007), in which 1D models were employed to simulate floods in urban areas with complex terrains.

We also note here the mapped inundation area in Betsholtz and Nordlöf (2017) for the flood event of the Höje River in Sweden, indicating that if the objective is solely to generate a flood extent map and none of other flow characteristics, e.g. velocity, is of importance, sufficient accuracy in generating

such a map can be achieved using the HEC-RAS 1D model without extensive calibrations. This is true whenever the floodplains are of a V-shape. We also experienced the same for the narrow river sections upstream, for which the 1D model can compute the inundation boundary properly. However, our results reveal that the 1D model cannot provide adequate accuracy for the inundation extent map for the coastal areas downstream. This is due to the 1D model's inability to simulate the dynamics of inundation, which in our case is of rapidly varying unsteady flow (RVUF) type. Unlike the case of Betsholtz and Nordlöf (2017), the complex topography contours around the downstream area in this paper cannot be considered as a simple floodplain, to which a 1D model can be applied.

From Figure 9, it is obvious that the 2D model represents the flood inundation extent significantly better than the 1D model especially for the downstream area. This indicates that the 2D model can capture the inundation dynamics for a RVUF type. Following the technique proposed in Casulli (2009), the sub-grid approach in HEC-RAS 2D model, which can capture important topographical features on a sub-grid level while keeping a larger size of computational grids, is proven effective and accurate for predicting the flood extent map. A similar accuracy with the 2D model is also shown by the coupled 1D–2D model in yielding the flood extent map. This can be achieved by selecting a proper combination of the computational domain for such a coupled modeling.

In Betsholtz and Nordlöf (2017), it was noted that implementing a coupled 1D–2D method for a V-shaped area might present issues, as it does not provide a distinct division between the primary channel, which ought to be modeled in 1D, and the floodplain. For dominantly V-shaped, narrow sections water flows (in the direction of the stream), a combined 1D–2D approach is often not required to create a computational domain. In other words, a 1D approach is already sufficient for such areas. This was accordingly the reason why we selected the domain configuration for our coupled 1D–2D model like that, namely, 1D for the narrow sections upstream and 2D for the coastal areas downstream, but not vice-versa and not to create 1D–2D domains

along the narrow river sections upstream. Notwithstanding, we believe that even if 1D–2D domains are created for the upstream area and 2D domains for the downstream one, a similar result with that of coupled 1D–2D model already shown in Figure 9 may be expected.

5.2 Flow Exchanging in 1D–2D Interface

All the aforementioned results signify similarities in the flood extent map between coupled 1D–2D and 2D models but with significantly different computational time. Now, this raises a question about the numerical treatment of flow exchanging between 1D and 2D domains at their interface. As noted in Betsholtz and Nordlöf (2017), there are two options for establishing the interface between 1D and 2D models, namely either by using a lateral connection or directly connecting 1D cross-section data with a 2D area.

In the first option, lateral structures are employed at the interface. So, whenever water level in the 1D cross section or 2D area is higher than the level of the lateral structures, the flow can be calculated in two ways, namely by a weir flow formula or by solving the 2D shallow water equations (USACE, 2016). If the weir flow formula is used, then the flow is calculated using a weir equation, which is thereafter considered as a unit discharge (a boundary condition for the variables u and/or v in Equation (7) and Equation (8) for a cell flux of the 2D model. If solving the 2D shallow water equations is chosen, then the 1D water surface profile is considered as a stage boundary condition to the corresponding 2D cell fluxes.

Since our case study involves completely different regions between upstream (the V-shaped, narrow river sections) and downstream (the floodplains of coastal areas), we opted for the second option by directly connecting the 1D cross-section data (upstream) with the 2D computational domain (downstream). As pointed out in Betsholtz and Nordlöf (2017), the discharge from the 1D model is distributed into the 2D model according to the conveyance distribution in the associated cross-section. However, to the best of our knowledge, there is no clear guidance on how these computations are processed in HEC-RAS, for instance, whether the flow can be in both directions (1D to 2D and 2D to 1D).

It was observed in Dasallas et al. (2019) that HEC-RAS with coupled 1D–2D model demonstrated an inconsistent increase in the flooded area: at 7 hours after the levee breach, 75% of the total area is flooded, and this increases to 97% after 16 hours. They presumed the possible reason was due to the numerical treatment for the interface of the 1D and 2D domains, which allowed for immediate interactions between the 1D and 2D flow components within the hydraulic linkage structure. However, this has not been proven yet. Despite such an inconsistent increase, they noted that the results of HEC-RAS coupled 1D–2D model were deemed more realistic than others (Gerris and FLUMEN models) with respect to the ideal behavior of flood dynamics. Unlike in Dasallas et al. (2019), we did not observe in our study any inconsistencies in the increase of the flooded area by the coupled 1D–2D model (when compared to the 2D model).

We also note here another finding of Betsholtz and Nordlöf (2017), where the coupled 1D–2D model was found to be very sensitive to time step and 1D–2D iterations (this is the option available in HEC-RAS for the 1D–2D solver). They showed that employing a small time step and utilizing 1D–2D iterations could reduce the numerical oscillations but with an increase in computational time. They also explored that the results of solving the 2D shallow water equations at the 1D–2D interface were more sensitive to time step than those of calculating a weir equation. In their study, the coupled 1D–2D model suffered the most from stability issues, while the 2D model encountered the least stability problems. This finding is in accordance with our study, as we experienced a dramatic increase of computational time for the coupled 1D–2D model. Additionally, we also found that this model had stability issues, thus requiring many 1D–2D iterations to stabilize.

5.3 Uncertainties of Modeling

A discussion remains regarding any of the uncertainties involved in our simulations. Based on

Beven et al. (2018), uncertainties of hydraulic modeling may be caused by several reasons, e.g. model structure, model input, model parameters, and the modeler. In this section, we identify the source of uncertainties to be model input and model parameters. The former emerges from the DEM, breach outflow, and downstream boundary condition as the inputs for our model, while the latter is related to the Manning coefficients employed in our simulations.

We understand that it is desirable, whenever feasible, to acquire fine-resolution measurements of topographic and photogrammetry data, so that any modeling uncertainties emerging from this basic input can be avoided. However, it is often not possible to obtain such fine-resolution data, especially for data-sparse regions like Indonesia. Hence, using DEM as an input for hydraulic modeling is inevitable. While satellite-derived DEMs are available from many open-access sources and have become more common, they are typically of coarse-resolution, within ~90 m to ~30 m. In this study, we employed ALOS with ~30 m resolution. This resolution is perhaps quite coarse to capture the existence of hydraulic structures like piers, bridges, gates, etc., and thus being neglected in our study. Note that these coarse-resolution DEM and land use map may also be considered the main limitation in our study.

Indeed, there is another open-access DEM source for our case study, namely DEMNAS (DEM Nasional) with a resolution of ~8.1 m. However, it was not appropriate for our dam-break simulations. According to Julzarika and Harintaka (2019), DEMNAS tends to represent most regions of Indonesia in the form of Digital Surface Model (DSM) and only a small portion as Digital Terrain Model (DTM). Note that for dam-break modeling, DTM data is required, whereas using DSM may misinterpret the modeling results. In Ginting et al. (2024), it was emphasized that utilizing DEMs of a finer resolution does not necessarily yield more accurate results compared to DEMs of a coarser-resolution.

Another uncertainty regarding model input is the breach outflow hydrograph computed with parametric models, which use regression analysis to predict the failure formation time and the breach geometry based on data from previous failure events. The results in Figure 4 are selected after a careful investigation by Kieswanti (2023) that comprehensively discussed some parametric models employed to estimate the breach outflow hydrograph for the Way-Ela dam-break event. While this approach may apply to estimating a final breach condition, the breach progression is in fact not known and, therefore, we assumed such a progression to be time-dependent linearly to the failure formation time. This was done in HEC-RAS with a simple routing procedure.

Another predictive method for estimating the breach outflow hydrograph is by means of physically based models that rely on the hydrodynamics, sediment transport equations, and soil mechanics principles to model the breaching process; for example, see Wu et al. (2012), in which a 2D model was used for overtopping breaching. Because the (detailed) physical models are computationally expensive, their simplified versions are thus commonly used in practices with certain simplifications and assumptions; see Zhong et al. (2016). Note that physically based breach modeling is currently applicable only to overtopping failures. Modeling breaches caused by piping, which involve both pipe and open-channel flows like those experienced during the Way-Ela dam-break event, continues to be a challenge.

The downstream boundary condition used in our simulations was an energy slope for the normal depth. In other words, the water surface fluctuations at the ocean due to tidal forcing were neglected. Hence, this issue raises uncertainty. Nevertheless, the effects of tidal fluctuations on the dam-break flood characteristics are insignificant. This was proven by specifying water level 2 m higher and lower than the elevation of the normal depth for the downstream boundary, where almost no differences in flow depth and velocity were observed. Lastly, we notice the uncertainty may arise due to the Manning coefficients. Since each land use type has a certain range of its Manning coefficient, we calibrated the values iteratively within that range until the simulated flood extent map agrees with the observed inundation area. The results in Table 4 are

in accordance with the findings in Ginting et al. (2024). In our work, we observed that the results are insensitive to the Manning coefficient values.

6. Conclusions

A comparison of 1D, coupled 1D–2D, and 2D models within the framework of HEC-RAS 6.3 software has been presented to simulate the Way-Ela dam-break event occurred in 2013 in Indonesia. Our study focused on assessing the accuracy of these models against the observed inundation area as well as their computational cost. An open-access, satellite-derived DEM, i.e. ALOS (~30 m), was used as the input. The breach outflow hydrograph was estimated using a parametric model following the Von Thun & Gillette formula.

Our results contribute to better understanding in choosing a suitable hydrodynamic model for dam-break simulations as a trade-off between accuracy and computational cost. Although the 1D model is shown to be very efficient, it entails several shortcomings in terms of accuracy (it fails to estimate the flood extent map for the coastal area) and stability (it produces oscillations for depth and velocity). In contrast, the 2D model can estimate the maximum inundation area accurately with a reasonable computation time.

While the coupled 1D–2D model is expected to outperform the efficiency of the 2D model, its computational time turns out to be significantly more expensive. Hypothetically, this is related to the numerical treatment at the 1D–2D domain interface. The coupled 1D–2D model can nevertheless provide a similar accuracy with the 2D model. We note that the 2D model should be used for dam-break simulations to yield accurate results with a reasonable computational time. However, considering that the constraints on the numerical treatments at 1D–2D interface will be fixed in the future, the coupled 1D–2D model may be regarded as a reliable approach to reducing the computational costs of the 2D model. Finally, we note that the coarse-resolution DEM and land use map used in our study can be considered as the main limitation for our analysis; it is therefore preferable to acquire fine-resolution topography and photogrammetry data to better represent the field condition so that more accurate results may be expected for future studies.

References

Awal, R., Nakagawa, H., Fujita, M., Kawaike, K., Baba, Y., Zhang, H. (2011). Study on Piping Failure of Natural Dam. *Journal of Japan Society of Civil Engineers* **67(4)**, 157-162. https://doi.org/10.2208/jscejhe.67.I_157.

Benazir, Triatmadja, R., Rahardjo, A.P., Yuwono, N. (2019). The Behavior of a Tsunami-like Wave Produced by Dam Break and its Run-up on 1:20 Slope. *Science of Tsunami Hazards* **38(2)**, 49-67.

Betsholtz, A., Nordlöf, B. (2017). Potentials And Limitations Of 1D, 2D, And Coupled 1D–2D Flood Modelling In HEC-RAS. Thesis, Lund University. https://www.lunduniversity.lu.se/lup/publication/8904721.

Bettiol, G.M., Ferreira, M.E., Motta, L.P., Cremon, É.H., Sano, E.E. (2021). Conformity Of the Nasadem_Hgt and ALOS Aw3d30 DEM with the Altitude from the Brazilian Geodetic Reference Stations: A Case Study from Brazilian Cerrado. *Sensors* **21(9)**, 2935. https://doi.org/10.3390/s21092935.

Beven, K.J., Almeida, S., Aspinall, W.P., Bates, P.D., Blazkova, S., Borgomeo, E., Freer, J., Goda, K., Hall, J.W., Phillips, J.C. (2018). Epistemic Uncertainties and Natural Hazard Risk Assessment–Part 1: A Review of Different Natural Hazard Areas. *Natural Hazard and Earth System Sciences* **18**, 2741-2768. https://doi.org/10.5194/nhess-18-2741-2018.

Bhola, P.K., Leandro, J., Disse, M. (2018). Framework for Offline Flood Inundation Forecasts for Two-Dimensional Hydrodynamic Models. *Geosciences* **8(9)**, 346. https://doi.org/10.3390/geosciences8090346.

BNPB (2013a). Sebagian Bendungan Way Ela Jebol. Available at: https://www.bnpb.go.id/berita/sebagaian-bendungan-way-ela-jebol (Accessed 12. 27. 23). (In Indonesian).

BNPB (2013b). Status Awas Waduk Way Ela di Maluku, 4.817 Jiwa Harus Siaga. Available at: https://bnpb.go.id/berita/status-awas-waduk-way-ela-di-

maluku-4-817-jiwa-harus-siaga (Accessed 12.27.23). (In Indonesian).

Casulli, V. (2009). A High-Resolution Wetting and Drying Algorithm for Free-Surface Hydrodynamics. International *Journal for Numerical Methods in Fluids* **60(4)**, 391-408. https://doi.org/10.1002/fld.1896.

Chinnarasri, C., Jirakitlerd, S., Wongwises, S. (2004). Embankment Dam Breach and Its Outflow Characteristics. *Civil Engineering and Environmental Systems* **21(4)**, 247-264. https://doi.org/10.1080/10286600412331328622.

Chymyrov, A. (2021). Comparison of Different DEMs For Hydrological Studies in The Mountainous Areas. The Egyptian *Journal of Remote Sensing and Space Sciences* **24(3)**, 587-594. https://doi.org/10.1016/j.ejrs.2021.08.001.

Cook, A.C. (2008). Comparison of One-Dimensional HEC-RAS with Two-Dimensional FESWMS Model in Flood Inundation Mapping. Thesis. Purdue University. https://web.ics.purdue.edu/~vmerwade/reports/2008_02.pdf.

Costa, J.E., Schuster, R.L. (1987). The Formation and Failure of Natural Dams, Open File Report, U.S. Geological Survey. https://doi.org/10.3133/ofr87392.

Chanson, H. (2006). Analytical Solutions of Laminar and Turbulent Dam Break Wave. River Flow 2006: Proceeding of International Conference on Fluvial Hydraulics, Taylor & Francis, London, 465-474.

Dasallas, L., Kim, Y., An, H. (2019). Case Study of HEC-RAS 1D–2D Coupling Simulation: 2002 Baeksan Flood Event in Korea. *Water* **11(10)**, 2048. https://doi.org/10.3390/w11102048.

Detik (2013). Bendungan Way Ela di Maluku Tengah Jebol, 1 Orang Tewas dan 32 Terluka. Available at: https://news.detik.com/berita/d-2314491/bendungan-way-ela-di-maluku-tengah-jebol-1-orang-tewas-dan-32-terluka (Accessed 2.27.24). (In Indonesian).

Dressler, R. (1954). Comparison of Theories and Experiments for the Hydraulic Dam-break Wave. Proceeding of International Association of Scientific Hydrology Assemblée Générale, Rome, Italy, 3(38), 319-328.

FEMA (2013). Federal Guidelines for Inundation Mapping of Flood Risks Associated with Dam Incidents and Failures, Federal Emergency Management Agency, US Department of Homeland Security, Washington D.C. https://www.fema.gov/sites/default/files/2020-08/fema_dam-safety_inundation-mapping-flood-risks.pdf.

Froehlich, D.C. (2008). Embankment Dam Breach Parameters and Their Uncertainties. *Journal of Hydraulic Engineering* **134(12)**, 1708-1721. https://doi.org/10.1061/(ASCE)0733-9429(2008)134:12(1708).

Froehlich, D.C. (1995). Embankment Dam Breach Parameters Revisited. Proceeding of the first International Conference sponsored by the Water Resources Engineering Division of the American Society of Civil Engineer, San Antonio, Volume 1, 887-891.

Gharbi, M., Soualmia, A., Dartus, D., Masbernat, L. (2016). Comparison of 1D and 2D Hydraulic Models for Floods Simulation on the Medjerda River in Tunisia. Journal of Materials and Environmental Science 7(8), 3017-3026.

Ginting, B.M. (2019). Central-Upwind Scheme for 2D Turbulent Shallow Flows Using High-Resolution Meshes with Scalable Wall Functions. *Computers & Fluids* **179**, 394-421. https://doi.org/10.1016/j.compfluid.2018.11.014.

Ginting, B.M., Ginting, H. (2020). Extension Of Artificial Viscosity Technique for Solving 2D Non-Hydrostatic Shallow Water Equations. *European Journal of Mechanics - B/Fluids* **80**, 92-111. https://doi.org/10.1016/j.euromechflu.2019.12.002.

Ginting, B.M., Lidyana, P., Christopher, C., Yudianto, D., Yuebo, X. (2024). Evaluating The Satellite-Derived DEM Accuracy with Rain-On-Grid Modeling for Flood Hydrograph Prediction of Katulampa Watershed, Indonesia. International *Journal of River Basin Management*, 1-18. https://doi.org/10.1080/15715124.2024.2312857.

Ginting, B.M., Lidyana, P., Christopher, C., Yudianto, D., Yuebo, X. (2023). Comparison of Flood Hydrograph Prediction Between Synthetic Unit Hydrograph Methods and Rain-On-Grid Model for Katulampa Watershed, Indonesia. *Acta hydrotechnica* **36(64)**, 81-94. https://doi.org/10.15292/acta.hydro.2023.05.

Ginting, B.M., Riyanto, B.A., Ginting, H. (2013). Numerical Simulation of Dam Break Using Finite Volume Method Case Study of Situ Gintung. Proceeding of 4th International Seminar of HATHI, Yogyakarta, 195-206.

Julzarika, A., Harintaka, (2019). Indonesian DEMNAS: DSM or DTM?. Proceeding of 2019 IEEE Asia-Pacific Conference on Geoscience, Electronics and Remote

Sensing Technology (AGERS), Jakarta, 31–36. https://doi.org/10.1109/AGERS48446.2019.9034351.

Kobayashi, D., Uchida, T. (2022). Experimental and Numerical Investigation of Breaking Bores in Straight and Meandering Channels with Different Froude Numbers. *Coastal Engineering Journal* **64(3)**, 442-457. https://doi.org/10.1080/21664250.2022.2118431.

Kieswanti, C. (2023). Comparison Of Several Breaching Empirical Formulas for Dam-Break Propagation Analysis of Way Ela Dam, Ambon, Indonesia. Thesis. Parahyangan Catholic University.

Liputan 6 (2019). Mengenang Tragedi Subuh Situ Gintung. Available at: https://www.liputan6.com/news/read/3926859 (Accessed 4.17.24). (in Indonesian).

Lorenzo, G.D., Macchione, F. (2014). Formulas for the Peak Discharge from Breached Earthfill Dams. *Journal of Hydraulic Engineering* **140(1)**, 56-67. https://doi.org/10.1061/(ASCE)HY.1943-7900.0000796.

Macdonald, T.C., Langridge-Monopolis, J. (1984). Breaching Characteristics of Dam Failures. *Journal of Hydraulic Engineering* **110(5)**, 567-586. https://doi.org/10.1061/(ASCE)0733-9429(1984)110:5(567).

Mark, O., Weesakul, S., Apirumanekul, C., Aroonnet, S.B., Djordjević, S. (2004). Potential and Limitations of 1D Modelling of Urban Flooding. *Journal of Hydrology* **299(3-4)**, 284-299. https://doi.org/10.1016/j.jhydrol.2004.08.014.

Nabilah, R.A., Sutjiningsih, D., Anggraheni, E., Murningsih, S. (2020). Dam Break Analysis of Situ Gintung Dam Collapse Reconstruction. IOP Conference Series: Earth and Environmental Science, Volume 599, 2nd International Conference on Green Energy and Environment, Bangka Belitung Islands, Volume 599. https://doi.org/10.1088/1755-1315/599/1/012064.

Patel, D.P., Ramirez, J.A., Srivastava, P.K., Bray, M., Han, D. (2017). Assessment of Flood Inundation Mapping of Surat City by Coupled 1D/2D Hydrodynamic Modeling: A Case Application of The New HEC-RAS 5. *Natural Hazards* **89**, 93-130. https://doi.org/10.1007/s11069-017-2956-6.

Rachmadan, L.C. (2014). Analisa Keruntuhan Bendungan Alam Way Ela dengan Menggunakan Program Zhong Xing HY21. Thesis. Brawijaya University. (In Indonesian). http://repository.ub.ac.id/id/eprint/142457.

Ritter, A. (1892). Die Fortpflanzung der Wasserwellen. Zeitschrift des Vereines Deutscher Ingenieure 36, 947-954. (In German).

Salahuddin, S., Maricar, F., Lopa, R.T., Hatta, M.P. (2021). Debris Flow Velocity Due to The Collapse of Natural Dam, Proceeding of the 5th International Symposium on Infrastructure Development, Makassar Volume 841. https://doi.org/10.1088/1755-1315/841/1/012015.

Sebastian, A., Juan, A., Bedient, P. B. (2022). Chapter 5 - Urban Flood Modeling: Perspectives, Challenges, and Opportunities. *Coastal Flood Risk Reduction* 47-60, https://doi.org/10.1016/B978-0-323-85251-7.00005-6.

Singh, K.P., Snorrason, A. (1984). Sensitivity of Outflow Peaks and Flood Stages to the Selection of Dam Breach Parameters and Simulation Models. *Journal of Hydrology* **68(1-4)**, 295-310. https://doi.org/10.1016/0022-1694(84)90217-8.

Suneth, M.N., Pattiselano, A.E., Adam, F.P. (2016). Strategi Adaptasi Ekologi (Studi Kasus Bencana Alam Way Ela di Desa Negeri Lima Kecamatan Leihitu Kabupaten Maluku Tengah). *Jurnal Agrilan* **4(2)**, 26-40. (In Indonesian).

Takaku, J., Tadono, T., Doutsu, M., Ohgushi, F., Kai, H., 2020. Updates Of Aw3d30' ALOS Global Digital Surface Model with Other Open Access Datasets. The International Archives of the Photogrammetry, *Remote Sensing and Spatial Information Sciences* **43**, 183-190. https://doi.org/10.5194/isprs-archives-XLIII-B4-2020-183-2020.

Tayefi, V., Lane, S.N., Hardy, R.J., Yu, D. (2007). A Comparison of One- And Two-Dimensional Approaches to Modelling Flood Inundation Over Complex Upland Floodplains. *Hydrological Processes* **21(23)**, 3190-3202. https://doi.org/10.1002/hyp.6523.

Tesema, T.A. (2021). Impact of Identical Digital Elevation Model Resolution and Sources on Morphometric Parameters of Tena Watershed, Ethiopia. *Heliyon* **7(11)**. https://doi.org/10.1016/j.heliyon.2021.e08345.

The Japan Aerospace Exploration Agency (JAXA) (2006). ALOS: Advanced Land Observing Satellite. Available at:

Lim M.: Comparison of 1D, coupled 1D–2D, and 2D shallow water numerical modeling for dam-break flow analysis of
Way-Ela dam, Indonesia – Primerjava 1D, povezanega 1D–2D modeliranja plitvih voda za analizo pretoka ob porušitvi
jezu Way-Ela, Indonezija
Acta hydrotechnica **37/66 (2024)**, 27–50, Ljubljana

https://www.eorc.jaxa.jp/ALOS/en/index_e.htm
(Accessed 12.10.23).

USACE (2023a). Hydrologic Engineering Center, HEC-RAS, 1D Vs. 2D Hydraulic Modeling. US Army Corps of Engineers, Davis, CA.

USACE (2023b). Hydrologic Engineering Center, HEC-RAS, HEC-RAS 2D User's Manual. US Army Corps of Engineers, Davis, CA.

USACE (2016). Hydrologic Engineering Center, HEC-RAS, River Analysis System Hydraulic Reference Manual. US Army Corps of Engineers, Davis, CA.

Uuemaa, E., Ahi, S., Montibeller, B., Muru, M., Kmoch, Al. (2020). Vertical Accuracy of Freely Available Global Digi-Tal Elevation Models (ASTER, AW3D30, MERIT, TanDEM-X, SRTM, and NASADEM). *Remote Sensing* **12(21)**, 3482. https://doi.org/10.3390/rs12213482.

Vojinovic, Z., Tutulic, D. (2009). On The Use of 1D and Coupled 1D–2D Modelling Approaches for Assessment of Flood Damage in Urban Areas. *Urban Water Journal* **6(3)**, 183-199. https://doi.org/10.1080/15730620802566877.

Von Thun, J.L., Gillette, D.R. (1990). Guidance on Breach Parameters. U.S. Bureau of Reclamation: Denver, CO, USA.

Wisyanto, Naryanto, H.S. (2022). Analysis of Landslides and the Formation of Way Ela Natural Dam, Negeri Lima, Leihitu, Central Maluku. *Jurnal Sains dan Teknologi Mitigasi Bencana* **16(2)**, 30-39. https://doi.org/10.29122/jstmb.v16i2.5391. (In Indonesian).

Wu, W., Marsooli, R., He, Z. (2012). Depth-Averaged Two-Dimensional Model of Unsteady Flow and Sediment Transport due to Noncohesive Embankment Break/Breaching. *Journal of Hydraulic Engineering* **138(6)**, 503-516. https://doi.org/10.1061/(ASCE)HY.1943-7900.0000546.

Xu, Y., Zhang, L.M. (2009). Breaching Parameters for Earth and Rockfill Dams. *Journal of Geotechnical and Geoenvironmental Engineering* **135(12)**, 1957-1970. https://doi.org/10.1061/(ASCE)GT.1943-5606.0000162.

Yakti, B.P., Adityawan, M.B., Hadihardaja, I.K., Suryadi, Y., Nugroho, J., Adi Kuntoro, A. (2019). Analysis of Flood Propagation and Its Impact on Negeri Lima Village Due to The Failure of Way Ela Dam. MATEC Web Conferences, Volume 270, 2nd Conference for Civil Engineering Research Networks, Bandung, Volume 270. https://doi.org/10.1051/matecconf/201927004011.

Yudianto, D., Ginting, B.M., Sanjaya, S., Rusli, S.R., Wicaksono, A. (2021). A Framework of Dam-Break Hazard Risk Mapping for A Data-Sparse Region in Indonesia. *International Journal of Geo-information* **10(3)**. https://doi.org/10.3390/ijgi10030110.

Zhong, Q., Wu, W., Chen, S., Wang, M. (2016). Comparison of Simplified Physically Based Dam Breach Models. *Natural Hazards* **84**, 1385-1418. https://doi.org/10.1007/s11069-016-2492-9.